LONG -TERM PRODUCT OF EVAPOTRANSPIRATION USING AVHRR IN THE KRISHNA RIVER BASIN, INDIA.

Pardhasaradhi Teluguntla[1*], Dongryeol Ryu[1], Biju George[1] and Jeffrey Walker[2]

[1]Department of Civil and Environmental Engineering
The University of Melbourne
[2]Department of Civil Engineering
Monash University
*Phone number: 03-83445596
p.teluguntla@pgrad.unimelb.edu.au

Abstract

The Krishna River Basin in India is the fourth-largest catchment in terms of drainage area. In recent years the Krishna River Basin has experienced dramatic hydrologic changes such as a steeply declining river discharge due to the expanded irrigation developments. To study the changes in the hydrology of the Krishna River Basin, a long-term time series of monthly evapotranspiration (ET) maps has been derived using remotely sensed observations from the Advanced Very High Resolution Radiometer (AVHRR). This paper deals with the methodology that is used for estimating spatially distributed ET and its validation. A historical monthly composite of the AVHRR data at 0.1-degree resolution (visible, near-infrared, and thermal infrared) from 1981 to 2001 was used to derive the variables (e.g., surface temperature, albedo, land use, etc.) required for the estimation of spatially distributed ET. The Surface Energy Balance Algorithm for Land (SEBAL) is used to estimate spatially distributed evapotranspiration by combining remotely sensed and ground based metrological data. Point measurements from meteorological stations were subsequently used for quantitative validation together with irrigation maps, rainfall records, and drought history for qualitative validation.

Introduction

The Krishna River Basin encompasses three large states, Karnataka, Maharashtra and Andhra Pradesh, being one of India's largest domestic waterways supplying water to 80 million people. It is also one of the most important food production areas in the country. In recent years the Krishna River Basin has been experiencing dramatic changes in its hydrology; especially river discharge is declining (Biggs *et al.,* 2007, Venot *et al.,* 2007) even though no significant changes in annual rainfall have been reported. Changes in evapotranspiration (ET) originating majorly from the water consumption for irrigation and industry, along with the development of water storage for the agricultural and industrial water consumption can cause substantial effects on river discharge. The water captured by hydrological structures such as dams and reservoir may change the patterns of the annual hydrological cycle (Haddeland et al., 2006; De Rosnay et al., 2003). Therefore, there is an increasing demand to investigate the impact of agricultural and industrial water consumptions on spatial and temporal patterns of the ET and its implications on the basin-scale hydrology and water resources. Average annual runoff to the ocean was 57 km^3 (29% of rainfall) before 1970's (pre irrigation period) at Vijayawada, which is the last measuring point in the basin located 105 km upstream of the river's outlet to the ocean (Biggs *et al.,* 2007). Dam construction and irrigation expansion continued rapidly. This resulted in a decrease in annual average discharge to less than 13 km^3 (nearly 7% of rainfall) by 1990-2001, despite no significant decrease in rainfall. The average annual discharge of 13 km^3 is only 22% of the pre-irrigation discharge to the ocean. The remaining 78% of the river discharge is consumed by irrigated agriculture in the basin. By 2003 there was almost no discharge to ocean. Therefore it is believed that the extra water is consumed by the crops to meet the evapotranspiration demand, and that evapotranspiration is likely responsible for the observed changes in hydrology.

Long-term spatially distributed evapotranspiration (ET) is an important input to study the recent temporal changes in the hydrology of the Krishna River Basin. While there are other long-term ET products available for the region, these products are typically derived based on land surface models. For example, the Global Land Data Assimilation System (GLDAS) provides ET at 1-degree resolution for the entire globe (http://disc.sci.gsfc.nasa.gov/hydrology). To date the only available remote sensing product for the Basin is the MOD16, a MODIS evapotranspiration product (Wood et al., 2007), but the product is only available from 2002 onwards. Consequently this paper generates a long term ET product from remotely sensed data for the Krishna River Basin using the 20year Advanced Very High Resolution Radiometer (AVHRR) data set. Surface Energy Balance Algorithm for Land (SEBAL) is used in this study to estimate actual evapotranspiration using the AVHRR data.

Description of data and the study area

The Krishna River Basin located in southern India lies between east longitudes 73º15'E to 81º20'E and north latitudes 13º05'N to19º20'N. Total geographical area of the basin is 258,912 km^2 (Source: CWC), being partly in

the states of Karnataka (113,235 km²), Andhra Pradesh (76,252 km²) and Maharashtra (69,425 km²). The river originates in the Western Ghats at an elevation of about 1337 m just north of Mahabaleshwar, about 64 km from the Arabian Sea, and flows for about 1400 km before outfalling into the Bay of Bengal. The principal tributaries joining Krishna are the Ghataprabha, the Malaprabha, the Bhima, the Tungabhadra, the Vedavathi and the Musi. The basin has been divided into 12 major sub-basins for national water resources assessment. The average annual rainfall is 800 mm (spatially varying from 500 mm to 2000 mm) and maximum temperature varies 20^0C to 42^0C, minimum temperature 8^0C to 30^0C. Cropping pattern occurs in three distinct crop seasons: Kharif during the monsoon (June-November), Rabi during post-monsoon (December-March) and a short summer season (April-May). The Kharif crops completely depend on monsoon rains and any change in time or intensity will affect the crop yield.

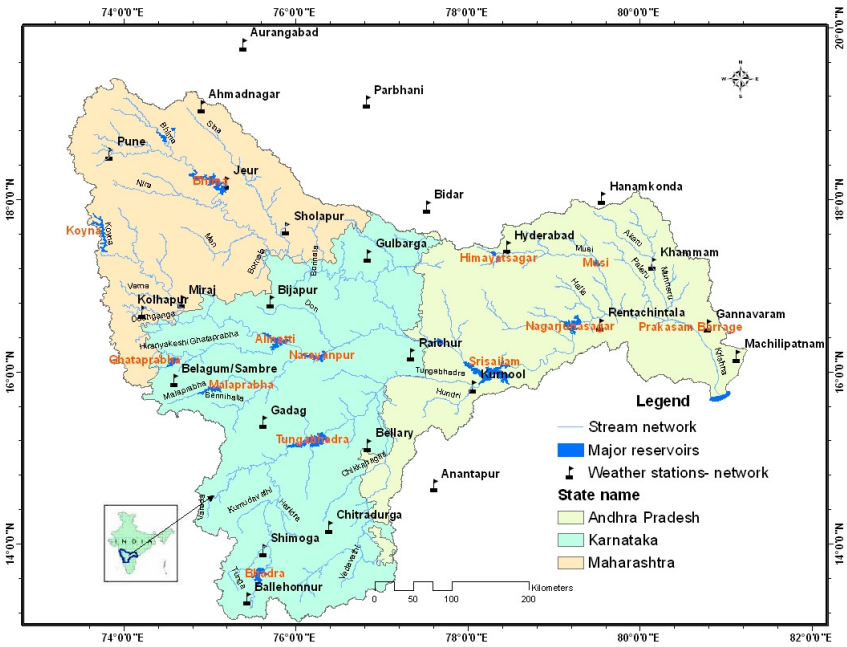

Figure 1: Location map of the Krishna River Basin, India showing state boundaries, river network major surface water reservoirs and weather stations (IMD) network.

A network of 24 meteorological stations(Figure 1) are maintained by the Indian metrological department (IMD) in the Krishna River Basin, with some additional meteorological stations maintained by research institutions such as International Crops Research Institute for Semi Arid Tropics (ICRISAT), Central Research Institute for Dry land Agriculture (CRIDA) and State Agriculture Department. Monthly-interpolated weather variables were generated using the Inverse Distance Weight (IDW) interpolation method from the available station data in the basin to calculate some of the required input parameters for SEBAL model.

The AVHRR timeseries satellite data for the Krishna River Basin was extracted from the calibrated global continuous time-series mega dataset (http://www.iwmidsp.org) composed of the individual files obtained from NASA

Goddard Space Flight Centre (www.daac.gsfc.gov/data/dataset/AVHRR). There are 239 months of data for each band, making a total of 956 bands from Band 1, 2, 4, and 5 for the entire basin. The characteristics of each band are listed in table.1. The monthly composites were generated through maximum value compositing (MVC) technique of the daily AVHRR data. The monthly composite data are superior to 10-day composites in terms of cloud free pixels (Wen and Tateishi, 2001).

Table 1 Characteristics of the AVHRR 0.1-degree datasets used for Krishna River Basin long-term evapotranspiration mapping

Band number (#)	**Wavelength range** (µm)	**Data final format** (%: for reflectance) (Kelvin: temperature)	**Range**
1	0.58-0.68	Reflectance(at-ground)	0-100
2	0.73-1.1	Reflectance(at-ground)	0-100
4	10.3-11.3	Brightness temperature	160-340
5	11.5-12.5	Brightness temperature	160-340

The original 16-bit scaled-reflectance is converted to percentage reflectance. Spectral information from visible (Band 1), near-infrared (Band 2), and thermal-infrared channels (Bands 4 and 5) are first converted into land surface characteristics such as surface albedo, vegetation index and surface temperature. The temperature of the surface as observed by satellites differs from actual surface temperatures due to the absorption and emission of thermal infrared radiance by the atmosphere. A split window technique can be used to adjust for this deviation and uses the difference in atmospheric attenuation between the 10.30–11.30 and the 11.50–12.50 µm spectrums (Kerr et al., 1992). Various formulations for the split window technique have been developed and tested by Pozo V´azquez et al. (1997). We used the split window equation developed by Price (1984), which has been reported to have an accuracy of 2–3 K:

$$T_s = T_4 + 3.33 * (T_4 - T_5) - 273.15 \ , \qquad (1)$$

where T_s (°C) is the surface temperature, T_4 (K) is the brightness temperature in AVHRR channel 4 and T_5 (K) is the brightness temperature in channel 5.

Normalized Difference Vegetation Index ($NDVI$) was estimated as:

$$NDVI = \frac{(Band2 - Band1)}{(Band2 + Band1)} \qquad (2)$$

where $Band2$ and $Band1$ are the spectral reflectance of the vegetated land surface in the near infrared and red bands of AVHRR.

Obtaining hot and cold pixels (anchor pixels) is an important step for the SEBAL-based ET estimation. Land-use /land-cover map is one of the important sources for identifying dry and wet classes to find hot and cold pixel values. These values will be used in SEBAL methodology.

Unsupervised classification using ISOCLASS cluster algorithm (ISODATA in ERDAS Imagine 8.6TM) followed by progressive generalization (Cihlar *et al*., 1998) was used to classify land use land cover classes with a maximum of 40 iterations and convergence threshold of 0.99. Using this methodology, 25 classes were generated. The unsupervised techniques is recommended for large areas that cover a wide but unknown range of vegetation types, and where landscape heterogeneity complicates identification of homogeneous training sites (Achard et al., 1995, Cihlar, 2000). Identification of training sites is particularly problematic for small, heterogeneous irrigated areas. In this study ISOCLASS clustering unsupervised classification was performed on yearly basis using two bands (layers) per month, 24 layers in total per year. The time-series data for each year run from June to May, which coincides with the start of the Kharif (June-Nov) cropping season. There were 25 classes obtained from the unsupervised classification which are merged using the class-average AVHRR NDVI time series, ground-truth data and GeoCover mosaics of Landsat imagery (Thenkabail *et al*., 2007, Tucker *et al*., 2004) and finally end up with 7 classes. To label the classes, we followed three approaches namely, tassel cap plots, space time spiral -spectral curves and NDVI time series plots and other sources of archive high resolution imageries.

Model Description

SEBAL a widely used remote sensing ET model for estimation of spatially distributed evapotranspiration. It is an intermediate approach using both empirical relationships and physical parameterizations formulated by Bastiaanssen *et al*. (1998a), which later has been evaluated by Bastiaanssen *et al*. (1998b) and Jacob *et al*. (2002). This model has been designed to calculate the energy partitioning at the regional scale with a minimum dependence on ground data.

SEBAL computes a complete radiation and energy balance along with the resistances for momentum, heat and water vapour transport for each pixel (Bastiaanssen et al., 1998a; Bastiaanssen, 2000). The key input data for SEBAL consists of spectral radiance in the visible, near infrared and thermal infrared part of the spectrum (band1, Band2, band4, band5 of AVHRR data). In addition to satellite images, the SEBAL model requires weather data parameters wind speed, humidity, solar radiation and air temperature.

The primary basis for the SEBAL model is the surface energy balance. The instantaneous latent heat flux is calculated for each pixel of the image as a 'residual' of the surface energy budget equation.

$$\lambda E = R_{\mathrm{n}} - \left(G_0 + H\right), \qquad (3)$$

where λE is the latent heat flux, R_n is the net radiation, G_0 is the soil heat flux and H is the sensible heat flux.

The latent heat flux describes the amount of energy consumed to maintain a certain crop evaporation rate. The surface albedo, surface temperature and vegetation index are derived from satellite measurements, and are used together to solve R_n, G_0 and H. The instantaneous latent heat flux (λE), is the calculated residual term of the energy budget, and it is then used to compute the instantaneous evaporative fraction (Λ):

The evaporative fraction is computed from the instantaneous surface energy balance at satellite overpass on a pixel-by-pixel basis

$$\Lambda = \frac{\lambda E}{\lambda E + H} = \frac{\lambda E}{R_{\mathrm{n}} - G_0} \tag{4}$$

The instantaneous evaporative fraction *expresses* the ratio of the actual to the crop evaporative demand when the atmospheric moisture conditions are in equilibrium with the soil moisture conditions. The instantaneous value can be used to calculate the daily value because evaporative fraction tends to be constant during daytime hours, although the H and λE fluxes vary considerably. The difference between the instantaneous evaporative fraction at satellite overpass and the evaporative fraction derived from the 24-hour integrated energy balance is marginal and may be neglected for time scales of 1 day or longer, G_0 can be ignored. The most important assumption of SEBAL is that the evaporative fraction is constant during the day. For periods longer than one day it may be assumed that the soil heat flux equals to zero. Consequently, at daily timescales evapotranspiration ET_{24} (mm/day) is calculated from the instantaneous evaporative fraction Λ, and the daily averaged net radiation.

$$ET_{24} = \frac{86400 \times 10^3}{\lambda\, \rho_{\mathrm{w}}} \Lambda\, R_{\mathrm{n24}}, \tag{5}$$

where R_{n24} (W/m^2) is the 24-h averaged net radiation, λ (J/kg) is the latent heat of vaporization, and ρw (kg/m^3) is the density of water.

Estimation of correction factor to account for cloudy days

Scaling up from daily ET estimates (ET_{24}) to monthly estimates is one major issue in this study. Because the satellite data used in this study are monthly maximum value composites from daily data. That means reflectance values are obtained from clear sky days, and so it gives maximum surface temperature value and hence maximum daily evapotranspiration for the month. To up scale from these daily estimates to monthly estimates, it is essential to consider rainy and/or cloudy days, other wise the estimates reflects clear sky conditions only. To account for cloudy conditions, a correction factor was estimated from weather stations daily data.

The correction factor was estimated with the following equation

$$ETcorrection = \frac{D1 * ET1 + D2 * ET2}{(D1 + D2) * ET2} \quad (6)$$

where $D1$ = no of rainy days in a month

$D2$ = no of clear sky days in a month

$ET1$ = Average reference ET of $D1$

$ET2$ = Average reference ET of $D2$

The FAO-56 Penman-Monteith formula was applied to calculate the reference ET by using daily meteorological data (minimum, maximum air temperature, relative humidity, wind speed and sun shine duration hours) for the stations with daily data. Consequently, the estimated SEBAL ET_{24} was multiplied by the correction factor to obtain corrected average 24hour (daily) actual ET from monthly data.

Results and Discussions

Daily actual evapotranspiration was estimated using AVHRR MVC satellite images and meteorological data for the period 1981-2001 with SEBAL by solving the energy balance equation for whole Krishna River Basin. The estimated actual evapotranspiration maps (Figure 2) clearly indicate the spatial patterns of different land use classes. Especially during the non monsoon season a clear differentiation was observed in the patterns of wet-area classes, such as irrigated agriculture command areas and forests against dry classes such as dry land rain-fed agriculture (Figure 2 and Figure 3). Even though the resolution of the image is coarser, the average daily evapotranspiration map shows the significant spatial variability. It is observed that during the monsoon season the variation of evapotranspiration between the pixels of the images are low. This may be due to the rainfall and soil moisture conditions. During non-monsoon months the variation of ET values between the pixels of the image are very high; pixels of forest areas and irrigated agriculture command area show high ET values (Figure 3), followed by supplemental irrigated area pixels, with the dry and rainfed agriculture classes showing low values.

As the images used in this study were monthly maximum value composites, it is observed that the average daily SEBAL ET estimates are relatively a little bit higher (Figure 2) during monsoon months. To account the rainy days, a correction factor (Eq.6) was implemented using daily weather data variables and applied in this study. ET correction factor was calculated with the available stations data. It is observed that the estimated correction factor was high during monsoon season and low during non monsoon season, it is obvious because of number of rainy days are high during monsoon months.

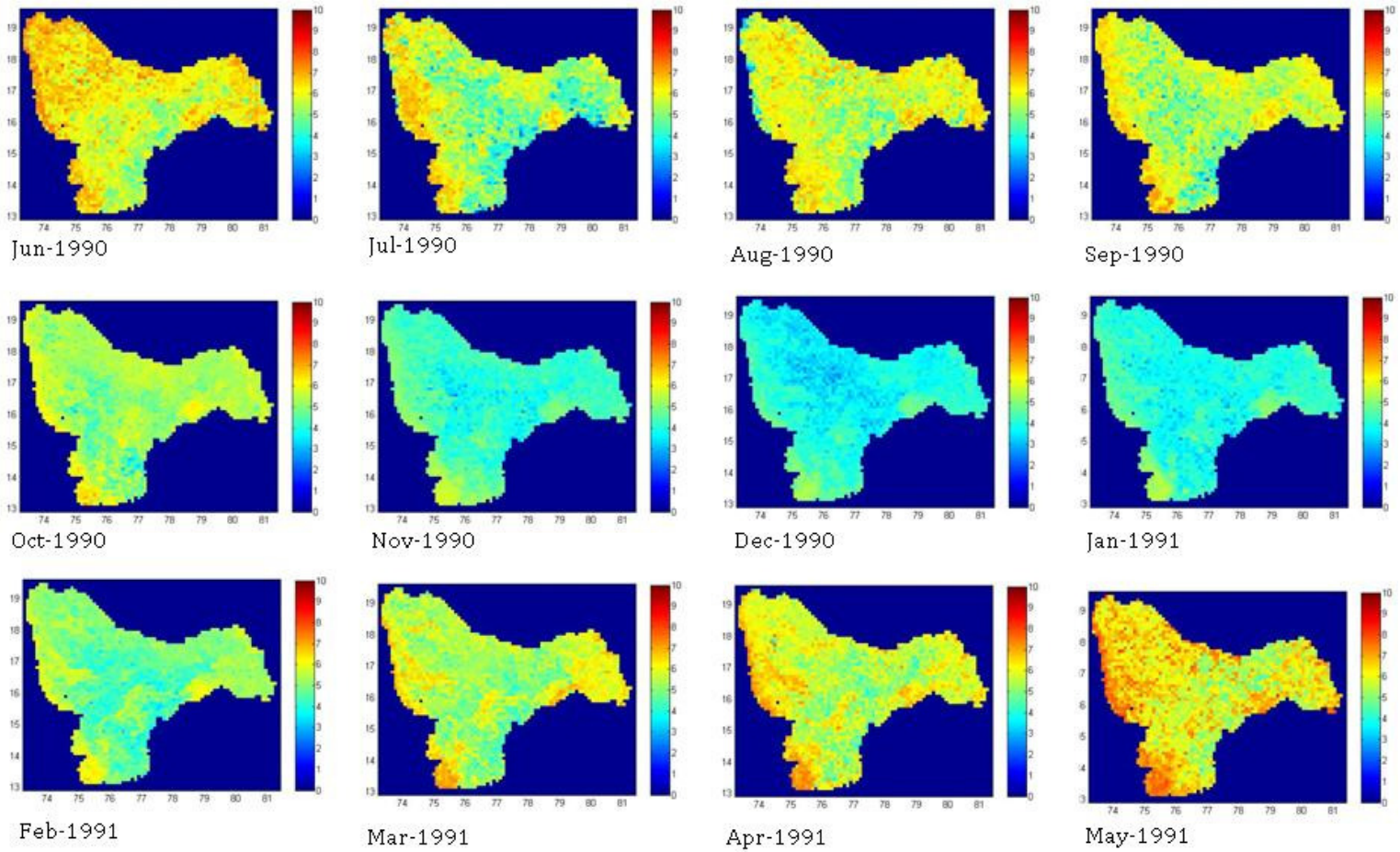

Figure 2: Estimated SEBAL actual average daily evapotranspiration from monthly MVC data for the year Jun1990 – May1991.

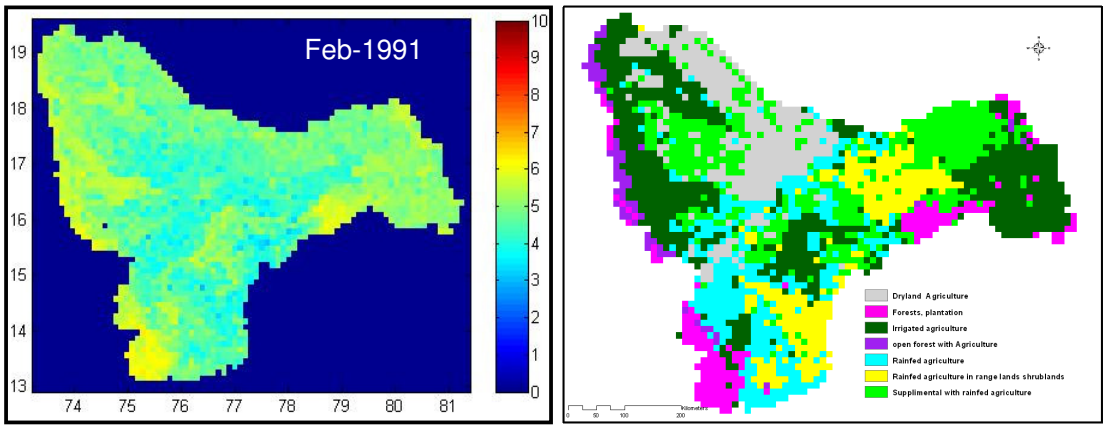

Figure 3: (a) Spatial distribution of evapotranspiration in February 1991(non monsoon season) and (b) Land-use /land-cover map of the Krishna River Basin.

To obtain the corrected evapotranspiration map, we have multiplied the actual ET estimated from SEBAL methodology with the correction factor. The corrected average daily (24h) actual evapotranspiration maps obtained show the seasonal variability (Figure 4) and temporal trend which follows the cropping seasons Kharif and Rabi. The climatology of three local meteorological stations data of the basin were used to analyse estimated SEBAL ET values. Pixels of the ET maps which are corresponding to the local weather stations (Hyderabad, Solapur and Bellary) were extracted from the estimated SEBAL ET maps.

The mean and standard deviation of 20 years SEBAL ET estimates of each month for the above three stations were summarised in Figure 5. The trend of three stations seems to be similar and showing with a clear seasonal variation but a little variation in its range of ET values.

The mean values of 20 years data for each month were taken from different sources of point measurements such as observed and pan evaporation and estimated reference potential evapotranspiration to compare with SEBAL estimates. The corrected SEBAL ET estimates were compared with pan-based evaporation and FAO-56 Penman-Monteith potential evapotranspiration (Figure 6). The graph of SEBAL ET shows the seasonal variability which is following the trend of pan evaporation. The correlation coefficient (R^2) between weighted (0.6) pan evaporation is ranging from 0.65 to 0.4 for the three stations. Some stations trend is correlating well with potential evapotranspiration and its R^2 value is ranging from 0.6 to 0.43.

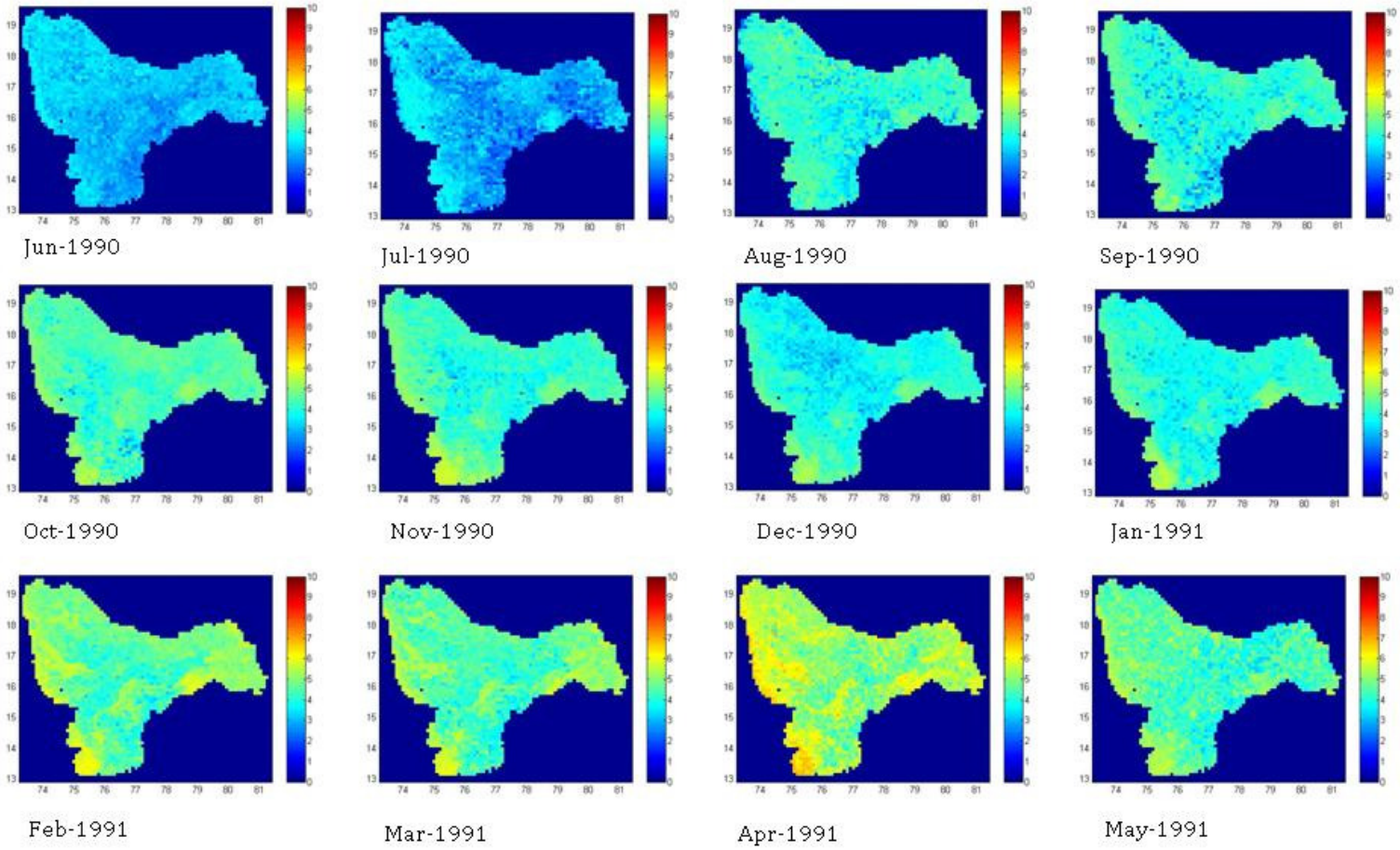

Figure 4: Corrected SEBAL average daily evapotranspiration from monthly MVC data for the year Jun1990 – May1991

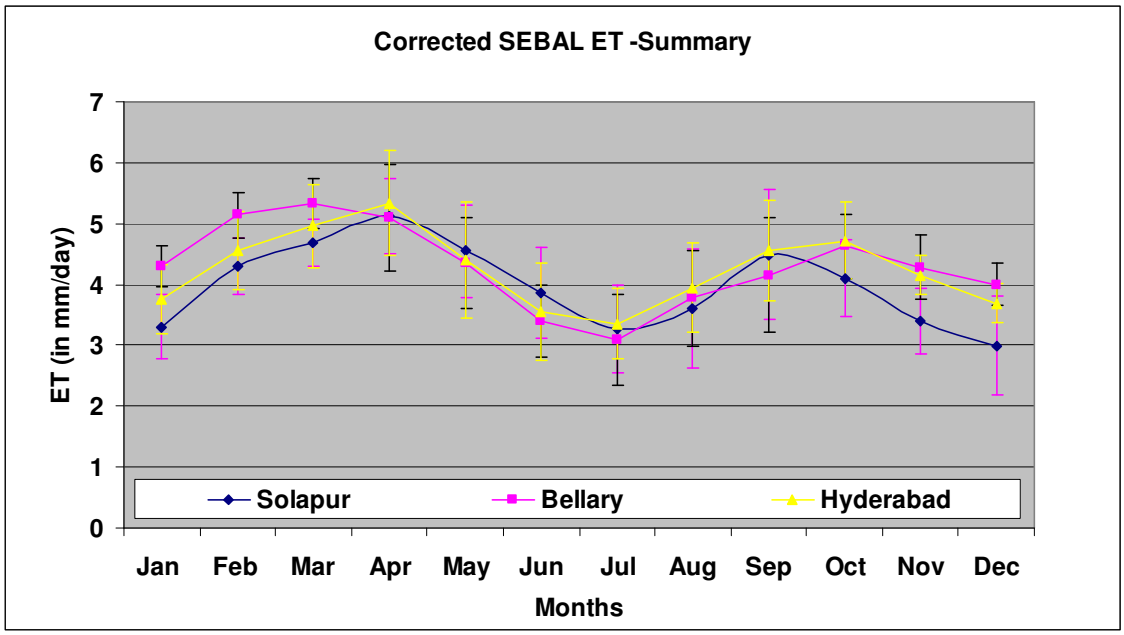

Figure 5: Long term (20 years) mean and standard deviation of monthly corrected SEBAL ET values of Solapur, Hyderabad and Bellary weather station locations.

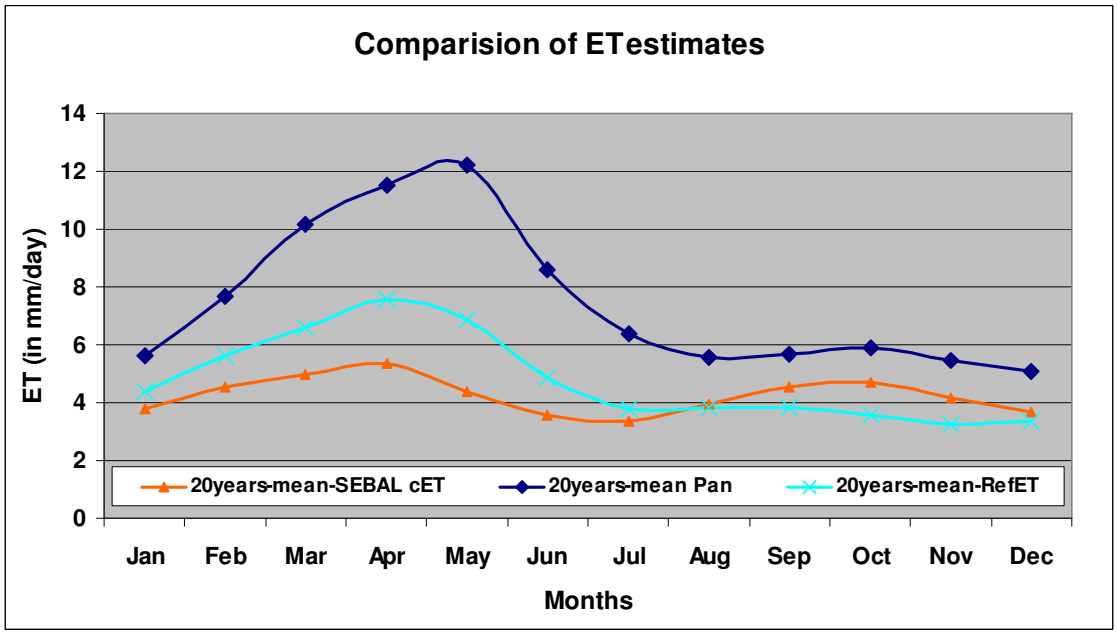

Figure 6: Comparison of corrected SEBAL ET estimates with point measurements pan evaporation and reference evapotranspiration of Hyderabad station.

Summary and Conclusions

The main purpose of this study was to develop a long term time-series of evapotranspiration maps to analyse spatial and temporal variations in the Krishna River Basin. The long-term ET maps for the Krishna River Basin were generated for the period 1981-2001 on a monthly basis. The results estimated from this study depict seasonal variations in ET. The SEBAL-based ET estimates from AVHRR show good correlation with the climatology of the local weather stations in the basin. The implementation of a cloudiness correction factor, which accounts for the ratio of clear vs. cloudy days of a month, has improved the monthly ET estimates from AVHRR. Comparison of the point measurements from meteorological stations with 10-km by 10-km grid cell values needs a refinement. It would be better to validate such a coarse resolution data with ET estimates from medium resolution and high resolution remote sensing data estimates rather than point measurements. This will be done in the future work of our study.

Acknowledgements

This research was funded with John All Wright Fellowship from the Australian Centre for International Agricultural Research (ACIAR). Weather data obtained from Indian Meteorological Department (IMD) and long-term AVHRR monthly composites data were obtained from the IWMIDSP. The authors would like to gratefully acknowledge the support of the ACIAR.

References

Allen, R., Pereira, L.A., Raes, D., Smith, M., 1998. Crop evapotranspiration; guidelines for computing crop water requirements, *FAO Irrigation and Drainage Paper No. 56,* FAO, Rome.

Bastiaanssen, W.G.M., M. Menenti, R.A. Feddes and A.A.M. Holtslag, 1998a. The Surface Energy Balance Algorithm for Land (SEBAL): Part 1 formulation, *International Journal of Hydrology*. 212-21: 198-212.

Bastiaanssen, W.G.M., Pelgrum, H., Wang, J., Ma, Y., Moreno, J.F., Roerink, G.J. & van der Wal, T. 1998b. A remote sensing surface energy balance algorithm for land (SEBAL): Part II Validation. *International Journal of Hydrology* 213–229.

Biggs TW, Gaur A, Scott CA, Gangadhararao, Parthasaradhi, Gumma, M.K, S. Acharya and H.Turral.2007. Closing of the Krishna basin: Summary of research, Hydronomic zones and water accounting. *IWMI Research Report 111*, Colombo: IWMI. 38p.

Cihlar, J., Ly, H., Xiao, Q., 1996. Land cover classification in AVHRR multichannel composites in Northern Environments. *Remote Sensing of Environment*. 58: 36-51.

Cihlar, J., 2000, Land cover mapping of large areas from satellites: status and research priorities. *International Journal of Remote Sensing*, 21**,** pp. 1093-1114.

Haddeland, I., Lettenmaier D. P., and Skaugen, T. 2006: Effects of irrigation on the water and energy balances of the Colorado and Mekong river basins, Journal of Hydrology., 324, 210–223.

International Water Management Institute's Data store house path way www.iwmidsp.org.

Kerr, Yann H.,Lagouarde, Jean Pierre,Imbernon, Jacques.,1992,Accurate land surface temperature retrieval from AVHRR data with use of an improved split window algorithm. *Remote Sensing of Environment,* 41, pp. 197-209.

Thenkabail, P., Parthasaradhi, G., Biggs, T.W., Gumma, M.K. and Turral, H., 2007.Spectral Matching Techniques to Determine Historical Land use/Land cover (LULC) and Irrigated Areas using Time-series AVHRR Pathfinder Datasets in the Krishna River Basin, India. *Photogrametric Engineering & Remote Sensing,* 73(9): 1029-1040.

Thenkabail, P.S., Biradar, C.M., Noojipady, P, Dheeravath, V., Li, Y.J., Velpuri, M, Gumma,M., Reddy, G.P.O., Turral, H., Cai, X.L., Vithanage, J.; Schull, M., Dutta, R,2008. Global Irrigated Area Map (GIAM) for the End of the Last Millennium Derived from Remote Sensing. *International Journal of Remote Sensing.*

Tucker, C.J., Grant, D.M., Dyktra, J.D. 2004. NASA's Global Orthorectified Landsat Data set. *Photogrammetric Engineering and Remote Sensing*. 70(3):313-322.

Venot, J.P, Turral,H Samad,M,Molle,F,2007.Shifting Waterscapes: Explaining Basin Closure in the Lower Krishna Basin, SouthIndia: *IWMI Research Report* 121, Colombo: IWMI.

Wen, C. G., and Tateishi, R, 2001. 30-second degree grid land cover classification of Asia. *International Journal of Remote Sensing*. 22 (18): 3845–3854.

Wood,E.F.,Vinkollu,R.K.,Fergusun,C.,Pinker,R.T.,Running,S.W.,Wang,H.2007 . The NASA Earth Observing System (EOS) Eapotranspiration Product: the New MOD16.*American Geophysical Union, Fall Meeting.* Abstract #H31I-06.